RESEARCH ARTICLE

Silica Gel for Enhanced Activity and Hypochlorite Protection of Cyanuric Acid Hydrolase in Recombinant *Escherichia coli*

Adi Radian,[a,b] Kelly G. Aukema,[a,c] Alptekin Aksan,[a,b] Lawrence P. Wackett[a,c]

BioTechnology Institute, University of Minnesota, St. Paul, Minnesota, USA[a]; Department of Mechanical Engineering, University of Minnesota, Minneapolis, Minnesota, USA[b]; Department of Biochemistry, Molecular Biology and Biophysics, University of Minnesota, St. Paul, Minnesota, USA[c]

ABSTRACT **Chlorinated isocyanuric acids are widely used water disinfectants that generate hypochlorite, but with repeated application, they build up cyanuric acid (CYA) that must be removed to maintain disinfection. 3-Aminopropyltriethoxysilane (APTES)-treated *Escherichia coli* cells expressing cyanuric acid hydrolase (CAH) from *Moorella thermoacetica* exhibited significantly high CYA degradation rates and provided protection against enzyme inactivation by hypochlorite (chlorine). APTES coating or encapsulation of cells had two benefits: (i) overcoming diffusion limitations imposed by the cell wall and (ii) protecting against hypochlorite inactivation of CAH activity. Cells encapsulated in APTES gels degraded CYA three times faster than nonfunctionalized tetraethoxysilane (TEOS) gels, and cells coated with APTES degraded CYA at a rate of 29 μmol/min per mg of CAH protein, similar to the rate with purified enzyme. UV spectroscopy, fluorescence spectroscopy, and scanning electron microscopy showed that the higher rates were due to APTES increasing membrane permeability and enhancing cyanuric acid diffusion into the cytoplasm to reach the CAH enzyme. Purified CAH enzyme was shown to be rapidly inactivated by hypochlorite. APTES aggregates surrounding cells protected via the amine groups reacting with hypochlorite as shown by pH changes, zeta potential measurements, and infrared spectroscopy. APTES-encapsulated *E. coli* cells expressing CAH degraded cyanuric acid at high rates in the presence of 1 to 10 ppm hypochlorite, showing effectiveness under swimming pool conditions. In contrast, CAH activity in TEOS gels or free cells was completely inactivated by hypochlorite. These studies show that commercially available silica materials can selectively enhance, protect, and immobilize whole-cell biocatalysts for specialized applications.**

IMPORTANCE **Hypochlorite is used in vast quantities for water disinfection, killing bacteria on surfaces, and washing and whitening. In pools, spas, and other waters, hypochlorite is frequently delivered as chlorinated isocyanuric acids that release hypochlorite and cyanuric acid. Over time, cyanuric acid accumulates and impairs disinfection and must be removed. The microbial enzyme cyanuric acid hydrolase can potentially remove cyanuric acid to restore disinfection and protect swimmers. Whole bacterial cells expressing cyanuric acid hydrolase were encapsulated in an inert silica matrix containing an amine group. The amine group serves to permeabilize the cell membrane and accelerate cyanuric acid degradation, and it also reacts with hypochlorite to protect against inactivation of cyanuric acid hydrolase. Methods for promoting whole-cell biocatalysis are important in biotechnology, and the present work illustrates approaches to enhance rates and protect against an inhibitory substance.**

Received 1 September 2015 **Accepted** 13 October 2015 **Published** 3 November 2015

Citation Radian A, Aukema KG, Aksan A, Wackett LP. 2015. Silica gel for enhanced activity and hypochlorite protection of cyanuric acid hydrolase in recombinant *Escherichia coli*. mBio 6(6):e01477-15. doi:10.1128/mBio.01477-15.

Editor Janet K. Jansson, Pacific Northwest National Laboratory

Address correspondence to Lawrence P. Wackett, wacke003@umn.edu.

This article is a direct contribution from a Fellow of the American Academy of Microbiology.

Enzyme catalysts generally display higher rates and specificity than conventional industrial catalysts do, but purified enzymes are often too fragile and/or expensive for many applications, necessitating creative methods for using whole-cell catalysts expressing the enzyme of interest (1). The use of whole bacterial cells and cells encapsulated in solid matrices can protect cytoplasmic enzymes against harsh conditions and greatly lower production costs. However, the cell membrane and encapsulating matrix can also significantly lower catalytic rates by limiting the diffusion of a substrate(s) to the enzyme inside the cell, and low-molecular-weight inhibitors may still permeate the cell and inactivate enzymes (1, 2).

One application in which purified enzymes would be prohibitively expensive and prone to inactivation is for the catalytic removal of cyanuric acid (CYA) from pools, spas, and fountains that use chloroisocyanuric acids for disinfection (3, 4). The chlorinated cyanuric acids deliver hypochlorite, which dismutates over time, requiring repeated additions of chlorinated cyanuric acids (4). CYA builds up after multiple additions because, unlike the hypochlorite, it is very stable chemically and does not degrade in the absence of enzymes. Studies dating back to the 1960s have demonstrated that high concentrations of CYA in pools significantly reduce disinfection efficacy, and thus, viruses, bacteria, and protozoa that may enter the water will not be inactivated (5–7). Therefore, it is essential to remove CYA when the concentration rises above 1 mM (~100 ppm). To date, the remedy for high CYA

concentrations has been to drain and refill the pools, which is inefficient in terms of pool management and significantly increases freshwater usage.

A solution to this problem has recently been conceived and focuses on using a microbial enzyme, cyanuric acid hydrolase (CAH), to hydrolytically degrade CYA at near neutral pH and ambient pool temperatures (8–11). CAH enzymes do not require cofactors, only water is required as a cosubstrate, and the reaction they catalyze goes to completion at equilibrium. CAHs are uniquely microbial enzymes found in divergent bacterial phyla, and numerous homologs have been shown to express in recombinant hosts to yield soluble, highly active proteins (9). Nevertheless, adding purified CAH directly to pools would likely prove too costly and impractical, whereas an immobilized whole-cell treatment system could find efficient application.

However, the use of a whole-cell CAH biocatalyst for this application does have two major drawbacks: one is the decreased rates expected by imposing a membrane barrier between CYA in the water and the CAH enzyme in the cytoplasm of the cell. The second problem likely to be encountered is the sensitivity of cells, and enzymes within the cells, to oxidation by hypochlorite, which is known to cause widespread inactivation of enzymes (12–16). In addition, encapsulation of cells in a matrix can impose additional diffusion barriers for CYA to reach the CAH enzyme. Therefore, for practical usage, an immobilization system should allow facile diffusion of substrate through the matrix, facilitate diffusion across the cell membranes, and protect against hypochlorite inactivation. This study aimed to develop a whole-cell encapsulation system to address all of these issues.

Whole-cell encapsulation in solid mesoporous matrices has been extensively studied and used to provide physical/mechanical protection for applications in biocatalysis and biodegradation (17–19). Whole-cell encapsulation, for example, in silica matrices, protects bacteria from environmental factors, predation, and accidental release and can increase long-term stability of enzyme activities (20–24). Moreover, the biosilica material can be fabricated into different sizes and shapes or applied as a coating to meet different functional needs. Furthermore, if the desired reactions are hydrolytic, the enzyme(s) can function independently of other cellular machinery and the cell can be nonviable. However, whole cells encapsulated in silica typically show a reduction in biotransformation rates compared to nonencapsulated systems due to diffusion limitations through the silica gel matrix, and transfer rates through cell membranes to the cytoplasmic enzyme further diminish reaction rates compared to the use of purified enzymes (2, 22, 24).

In a recent study by Yeom et al., three different bacterial CAH enzymes were expressed in *Escherichia coli*, encapsulated in a tetraethoxysiloxane (TEOS) silica gel, and compared with respect to activity and storage stability (25). CAH from *Moorella thermoacetica* ATCC 39073 was found to be the optimum *in vivo* enzyme for practical purposes, and molded TEOS microspherical beads containing *M. thermoacetica* were tested in a laboratory-scale, flowthrough water filtration system. Although the system completely degraded CYA in a reservoir containing 10 mM CYA, kinetic analysis indicated that the system showed significant diffusional limitations. Moreover, when tested with swimming pool water, the CAH enzyme activity decreased as a function of increasing hypochlorite concentrations (25).

The present study demonstrated a solution to both diffusion limitation and hypochlorite inactivation by engineering a permeabilizing and protective encapsulation system. To accomplish this, 3-aminopropyltriethoxysilane (APTES), which is widely used as an adhesion promoter, coupling agent, and resin additive, was selected here as a precursor for the silica gel encapsulation matrix. The hypothesis was that by using a matrix containing sacrificial amine groups that can react with the strong oxidant hypochlorite, enzyme oxidation and inactivation would be delayed. Additionally, amine groups can interact with and permeabilize the cell membranes of Gram-negative bacteria such as *E. coli* (26–28), which in turn may enhance substrate transport to the enzyme. In total, these new methods provided a protective, reactive silica material that also allowed for facile substrate diffusion to the CAH enzyme inside the cell.

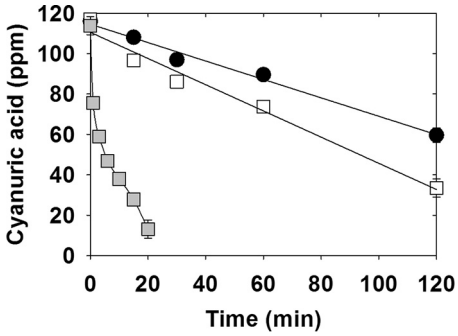

FIG 1 Comparison of cyanuric acid (CYA) degradation rates by cyanuric acid hydrolase (CAH) from *Moorella thermoacetica* expressed in *E. coli* and tested as cell extract, whole-cell, and encapsulated cell forms. The three treatments are 0.025 g of *E. coli* expressing CAH or the equivalent amount of cell-free CAH in the following: TEOS gel (black circles), freely suspended cells (white squares), or lysed cells (gray squares). The means ± standard deviations (error bars) of three replicate experiments were calculated, but the standard deviations are smaller than the symbols for most measurements and thus are not visible.

RESULTS AND DISCUSSION

In the current study, the cyanuric acid hydrolase (CAH) from *Moorella thermoacetica* was shown to efficiently degrade cyanuric acid in the presence of hypochlorite. To accomplish this, two major problems had to be overcome: (i) diffusion limitations brought on by encapsulating whole cells and (ii) sustaining CAH activity in the presence of disinfectant levels of hypochlorite. The two problems were examined separately, first diffusion and then hypochlorite resistance, and then combined and tested in experiments that simulated a disinfected water application.

Diffusion limitations. Initially, the effects of diffusion on CAH degradation were assessed by measuring the rate of enzymatic activity with comparable levels of CAH enzyme contained within TEOS-encapsulated cells, free cells in solution, and soluble CAH enzyme (Fig. 1). To make the data directly comparable, each sample contained 0.025 g of cells or the amount of enzyme contained within 0.025 g of cells.

The free, soluble enzyme was significantly faster than whole cells and TEOS-encapsulated cells (Fig. 1). The initial drop of CYA represents a rate of 1 to 2 orders of magnitude faster than free cells or TEOS-encapsulated cells, and thereafter, the rate falloff is likely due to the enzyme being only partly substrate saturated. The K_m value for the purified *M. thermoacetica* CAH was previously determined to be 110 μM (8). In contrast, there was a much more

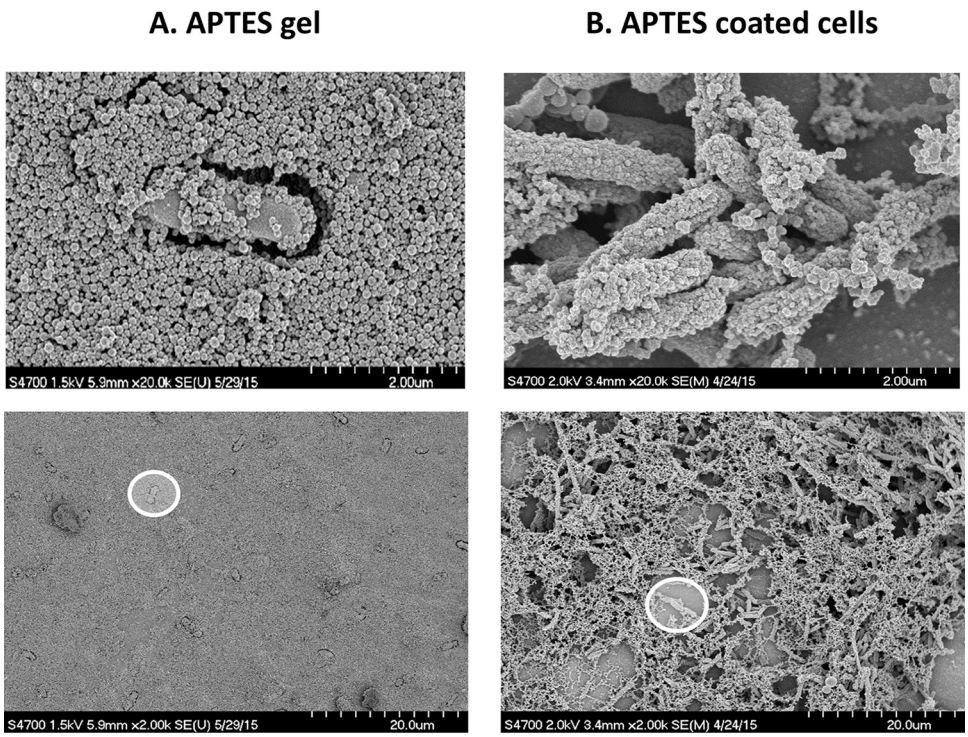

FIG 2 Scanning electron micrographs at two levels of magnification showing encapsulated *E. coli* cells in APTES gels with SNPs (APTES gel) (A) and *E. coli* cells coated by APTES (APTES-coated cells) (B). The scale bars of the top images are 2 μm, and the scale bars of the bottom images are 20 μm. Each white circle highlights a single cell to give another perspective of the size differences between the top and bottom images.

modest rate difference between the suspended and gel-encapsulated cells, with the free cells showing an approximately 1.4-fold-higher rate. The significant disparity in rate between free enzyme and either free cells or encapsulated cells suggested that the cell membrane is the major diffusional barrier for the substrate to reach the soluble CAH enzyme.

To overcome the diffusional barrier imposed by the cell membrane, a permeabilizing silica gel was developed. Previous studies have shown that appropriately positioned alkylamine functional groups disrupt Gram-negative cellular membranes, cause leakage of cytoplasmic materials, and render the bacteria nonviable (26–28). Since cyanuric acid-degrading enzymes use only water as a cosubstrate, cells expressing CAH can be nonviable and still show CYA degradation activity for weeks (25). In this context, a silica gel precursor with an amine functional group, 3-aminopropyltriethoxysilane (APTES), was chosen as the cross-linker for the silica gel matrix. Two treatments were applied to the cells to evaluate different levels of encapsulation in terms of diffusion and protection against hypochlorite inactivation. Figure 2A shows one approach in which APTES and silica nanoparticles (SNPs) were mixed to make a solid, continuous three-dimensional silica gel with the cells embedded within the gel. Figure 2B shows another process in which free cells were coated by particles formed by polymerization of hydrolyzed APTES that did not create a continuous gel but had a flake-like macrostructure. This was caused by cell clumping with a coated mesh-like appearance. The mesh would be expected to have a lower diffusional barrier than the gel, and it was expected that the amine groups on the APTES would render the membrane more porous.

The results of CYA degradation assays clearly demonstrated greatly enhanced activity of APTES-coated cells in comparison to APTES gels, with an approximately 7-fold-higher CYA degradation rate (Fig. 3). In fact, the rates were ~70% of the rate of a comparable level of free enzyme. Interpreting this in light of Fig. 1, these data suggested that the APTES coating was causing a significant enhancement in the diffusion of CYA through the bacterial membranes and into the cytoplasm of the cell where the CAH enzyme resides. Further evidence that the amine groups of APTES make membranes porous is derived from the observation that degradation of CYA by APTES gels was faster than that of free cells in solution or TEOS gels, consistent with the idea that APTES enhances substrate diffusion into the cytoplasmic CAH enzyme.

To assess whether APTES enhances reaction rates due to its increasing membrane permeability, the TEOS and APTES gels were compared with respect to movement of cellular material out of the cell and entry of fluorescent dyes into the cell. To determine leakage out of the cells, the gel plugs were gently shaken with 3 ml of phosphate-buffered saline (PBS), and an increase in absorbance at 280 nm was monitored as described in Materials and Methods. To monitor for a possible leakage of proteins, the PBS solution was loaded onto an SDS-polyacrylamide gel and stained as described in Materials and Methods. Previously, it had been shown that encapsulation of *E. coli* cells in TEOS gel causes some membrane disruption (30), consistent with the increase in absorbance at 280 nm observed here (Fig. 4A). However, leakage of absorbing material out of the cells was significantly greater for the APTES gels (Fig. 4A; see Fig. S1 in the supplemental material).

The results of the experiments with SDS gels suggested that only a small amount of CAH was present outside the cells, and therefore, most of the increase in absorbance at 280 nm can be

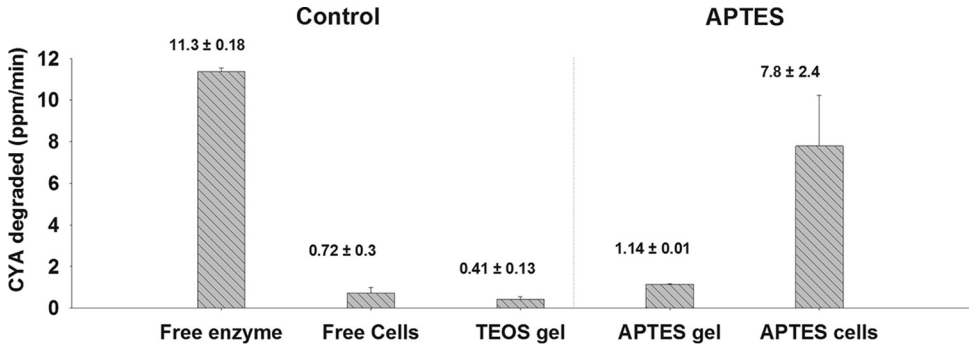

FIG 3 Comparison of cyanuric acid hydrolysis rates of free CAH enzyme, suspended *E. coli* (CAH) cells, TEOS gel, APTES gel, and APTES-coated cells. The different experimental treatments had comparable amounts of cells or cell material as described in Materials and Methods.

attributed to the leakage of low-molecular-weight molecules (see Fig. S1 in the supplemental material). This conclusion was supported by an experiment testing for enzyme activity leakage from the gels. An APTES gel containing *E. coli* cells expressing CAH was stored in buffer solution for a month. The buffer and gel plug were transferred to a fresh solution and assayed periodically. The CAH enzyme activity remained uniform with the gel, suggesting little or no leakage of the enzyme (Fig. S2).

Next, diffusion into the cells was determined with the probe propidium iodide (PI) (MW of 668), which is known to diffuse significantly only into membrane-disrupted cells, where it becomes intensely fluorescent by intercalating between DNA bases (31, 32). The cells were reacted for 10 min with TEOS or APTES and then centrifuged and washed prior to the addition of PI. The cells coated with APTES showed a nearly 10-fold-greater fluorescence intensity compared to cells coated with TEOS (Fig. 4B). Scanning electron microscopy (SEM) images of the cells mixed with TEOS or APTES also indicated that the cell membranes with APTES treatment were significantly misshapen (Fig. 4C). In addition to PI, we experimented with significantly larger molecules, fluorescently labeled dextrans with molecular weights (MWs) of 3,000 to 4,000 (33, 34). These larger molecules showed no evidence of diffusion into cells reacted with APTES or TEOS (data not shown), suggesting that the damaged membrane could mostly keep larger molecules from diffusing in. In total, the data suggested that both APTES-coated cells and APTES gels allow significant passage of small organic molecules in and out while largely or completely retaining molecules the size of enzymes within the cells and silica.

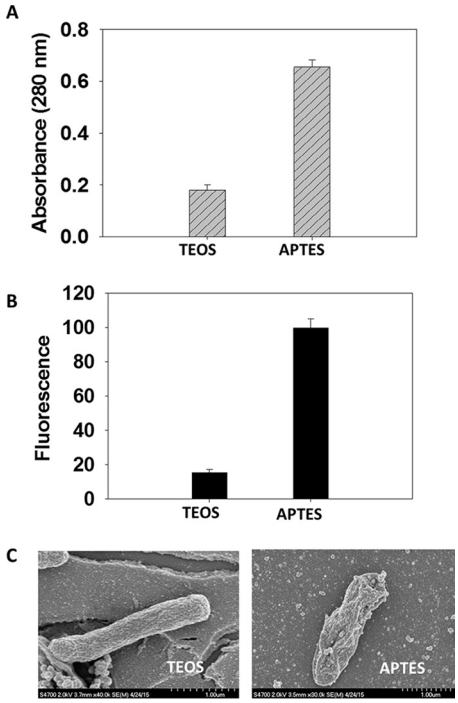

FIG 4 Experiments showing leakiness of APTES-treated cells compared to similar treatments with TEOS. The treatments are shown in the three panels as follows. (A) Measurement of cell material leaking out of the cell via absorbance at 280 nm with TEOS and APTES gel plugs shaken for 1 h in phosphate-buffered saline solution. (B) Measurement of relative fluorescence intensity (in arbitrary units) of cells treated with propidium iodide after agitation with TEOS or APTES. (C) Scanning electron microscopy images of *E. coli* cells after reacting with TEOS and APTES as described in Materials and Methods. Bars, 1 μm.

Hypochlorite inactivation of enzyme, free cells, and TEOS and APTES gels. The second major issue hindering the development of a robust biocatalytic system for CYA removal from swimming pool water is the sensitivity of the CAH enzyme to hypochlorite as shown in a previous study (25). In the experiments detailed below, relatively high levels of hypochlorite were used to accelerate oxidation processes and robustly challenge protection methods.

Figure 5 shows two studies investigating the detrimental effect of hypochlorite on CAH in which: (i) the enzyme is completely exposed to hypochlorite *in vitro* (Fig. 5A) and (ii) the enzyme is completely exposed to hypochlorite *in vivo* in free cells and cells encapsulated in silica gels (Fig. 5B). Figure 5A shows purified CAH enzyme in the absence of a cell or other materials that can react with hypochlorite to fully manifest the effects of hypochlorite. The CAH enzyme was rapidly inactivated, losing virtually all activity in less than 5 min at the highest concentration tested (744 ppm), and most of its activity was lost in less than an hour at a hypochlorite concentration of 74 ppm. Since these concentrations are much higher than typically found in pools, the purified enzyme was tested with 3 ppm, a typical disinfection concentration, and the enzyme activity was completely lost within 3 h, suggesting that the addition of purified CAH enzyme would be a poor option for treating chlorinated swimming pools (data not shown).

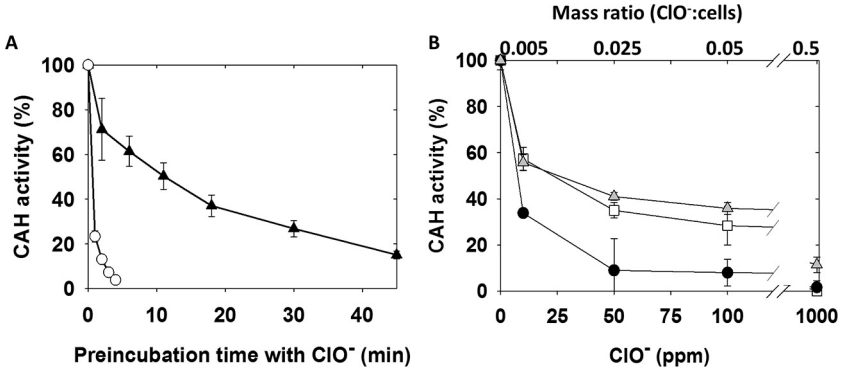

FIG 5 Detrimental effect of hypochlorite on the activity of CAH from *M. thermoacetica* with purified enzyme, free *E. coli* (CAH) cells, and *E. coli* (CAH) in TEOS and APTES gels. (A) Decrease in purified CAH enzymatic activity (as a percentage) following preincubation with 74.4 ppm hypochlorite (black triangles) and 744 ppm hypochlorite (white circles) at the times indicated prior to assay. (B) Decrease in activity (as a percentage) *in vivo* of 0.025 g *E. coli* (CAH) plotted versus the hypochlorite concentration (bottom *x* axis) or the mass ratio of hypochlorite to cells (wet weight) (top *x* axis). The three treatments are free cells (white squares), TEOS gel (black circles), and APTES gel (gray triangles). The activity was measured following a 1-h incubation with hypochlorite and 140 ppm CYA.

In the experiments shown in Fig. 5B, a comparison of the hypochlorite effect on whole cells and TEOS and APTES gels is shown. In a water treatment application, a critical component is the total amount of hypochlorite in relation to the total amount of reactive sites on the cell and the encapsulating matrix. We examined percent activity remaining after 1 h with only 2 mg of cells, which translates to only 0.03 mg of CAH enzyme. However, the whole cell offers thousands of proteins, DNA, and membrane components as targets for oxidation that compete with CAH for reactivity with hypochlorite, and thus, it provides some protection of CAH activity. This also means that more cells give more protection for a given amount of hypochlorite and that the ratio of hypochlorite to cell mass is important (top *x* axis).

Whole cells retained activity at relatively high hypochlorite concentrations and also showed significant resistance compared to cells encapsulated in TEOS gels. Previous studies showed that TEOS gels perturb *E. coli* membranes to some degree and that the membrane disruption allows greater diffusivity of external chemicals to reach cytoplasmic enzymes inside the cells (30). The present results suggested that hypochlorite can access the CAH enzyme more readily. Since we do not expect the TEOS-silica gel to react with hypochlorite, it does not offer protection, and so its effects are only detrimental. In contrast, the APTES-silica gel is protective. The cells in APTES gels are even slightly more resistant to hypochlorite than whole cells and retained some activity at 1,000 ppm hypochlorite (at a ClO^-/cell [wet weight] ratio of 0.5). This is not due to poorer diffusion into the cell because the earlier studies showed higher diffusivity into and out of cells and a higher *in vivo* CAH activity for cells treated with APTES. Since diffusivity is enhanced by APTES, yet the internal CAH enzyme is less vulnerable to hypochlorite, it was suggested that APTES itself protects against the detrimental effects of hypochlorite and that was investigated next by directly examining the expected reaction of the APTES amine groups with hypochlorite.

APTES reactions with hypochlorite. Based on known reactions between hypochlorite and alkylamines (35), it was hypothesized that each amine group on an APTES monomeric unit would react with two hypochlorite molecules and thus remove two reactive, oxidizing species from solution. APTES was polymerized into gels without bacteria and reacted with hypochlorite, and analytical measurements were done after adding hypochlorite up to a 3:1 molar ratio of hypochlorite to amine groups. The gel materials were analyzed by three different methods: pH determination (Fig. 6A), Fourier transform infrared spectroscopy (FTIR) (Fig. 6B), and zeta potential measurements (see Fig. S3 in the supplemental material).

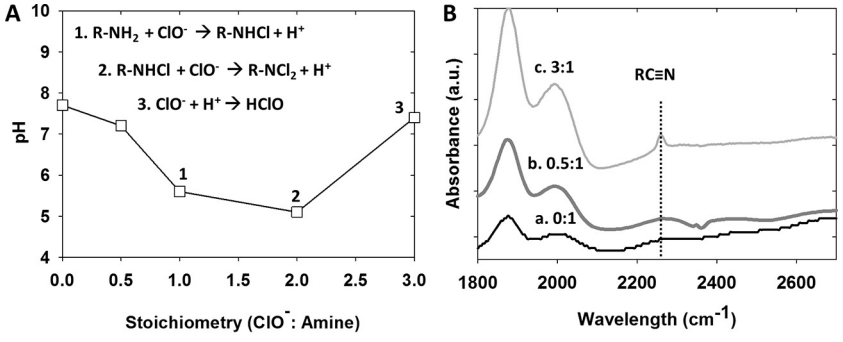

FIG 6 Reaction of the amino group on the APTES gels (without cells) with hypochlorite demonstrated by pH changes and amine oxidation by hypochlorite to a nitrile functionality. (A) pH measurements of APTES gel treated with hypochlorite (ClO^-) as a function of the ClO^-/amine stoichiometry. Known chemical reactions of ClO^- with amines are shown above the curve and indicate expected reactions with 1.0, 2.0, and 3.0 equivalents of ClO^-. (B) Fourier transform infrared spectroscopic (FTIR) analysis of APTES gels treated with ClO^- and excess NaOH (1 M) to promote nitrile formation at a stoichiometric ratio of hypochlorite to amine content of 0:1 (a), 0.5:1 (b), and 3:1 (c) in the gel. Absorbance is shown in arbitrary units (a.u.).

Amine oxidation reactions with hypochlorite are known to occur in two steps that each cause the displacement of a proton from the amine with the release of a proton, causing the lowering of the pH at each step (15, 36). At a 2:1 ratio of hypochlorite to amine groups, the pH is expected to be at its lowest point. The further addition of hypochlorite anion with a pK_a of 7.5 (36) to a solution at pH 5 (Fig. 6A) will cause essentially all excess hypochlorite anions to be protonated, effectively raising the pH again, and this was observed. Note that an exact pH titration cannot be made with these water-suspended gels because the hydroxyl-rich silica gel has a strong buffering capacity, and we cannot determine precisely how many free silica hydroxyl groups remain during the gelling process. Nevertheless, the pH trends clearly demonstrate that hypochlorite is reacting rapidly with APTES gels under the same conditions that the biological experiments were conducted.

Zeta potential experiments were consistent with the pH measurements and also illustrated the buffering capacity of the gel (see Fig. S3 in the supplemental material). APTES gel particles at pH 7.7 carry a negative zeta potential (−33 mV) due to the abundant hydroxyl groups. The addition of hypochlorite equivalent to one and then two times the molar equivalent of amine groups in the gel caused an increase in the zeta potential to −4.8 mV and +7.2 mV (±7), respectively. The protons released react with the negatively charged hydroxyl group on the gel and screen the negative charge of the particles. At hypochlorite concentrations three times the molar amine content, the zeta potential values are negative again (−38 mV) due to the excess of the negatively charged hypochlorite anion.

The pH and zeta potential measurements are consistent with the direct removal of reactive chlorine from solution by generating APTES chloramines, and FTIR experiments were conducted to observe these reactions. The sharpest and most distinct IR band that could be observed is a nitrile functionality and this can be generated from *N*,*N*-dichloroamines via a facile base-catalyzed dielimination, and that was done with NaOH to observe the nitrile band (Fig. 6B). Further details are described below. Amine groups have a distinct stretching band at 3,340 cm^{-1} and several bands between 1,610 and 1,460 cm^{-1} (37–39), but the broad Si-O (OH) bands at 3,500 cm^{-1} and 1,630 cm^{-1} (37, 40) largely mask the amines. Dichloroamines are inherently unstable and thus are not ideal to observe by FTIR, but their treatment with NaOH is known to convert them to nitriles (38). The aliphatic nitrile band (2,240 to 2,260 cm^{-1}) is apparent in a region not overlapping any siloxane vibrations (39, 41), and a distinct band was observed here at 2,250 cm^{-1}.

Simulated pool experiments. To test the applicability of the APTES-coated cells and the APTES gel, a larger scale experiment was designed to simulate conditions in an outdoor pool. Disinfection diminishes significantly at CYA concentrations at or above 100 ppm; therefore, water containing 100 ppm CYA and at a typical pool pH of 7.6 was remediated with different treatments to test different parameters. Each flask with 4 liters of water was treated with 40 mg (wet weight) of *E. coli* cells, either unencapsulated (free), encapsulated in APTES gel, or coated with APTES. In the first experiments, flasks did not contain hypochlorite. CYA degradation rates varied in the following order: APTES-coated cells > APTES gel > free cells (Fig. 7). This is in agreement with the batch experiments (Fig. 3) that showed a distinct advantage to the APTES-treated cells (both in the gel form and as coated cells) over the free cells. However, the significant difference in the rate of CYA degradation between APTES-coated cells and APTES gels is not as great as observed in the batch experiments (sevenfold difference). This is due to the application method of macroscale APTES gel plugs (Fig. 3) versus microparticles of the APTES gel dispersed in the solution (Fig. 7). The bioactivity of the dispersed gel microparticles is less diffusion limited; therefore, the rate of degradation is greater. Using known numbers for calculating soluble protein for *E. coli* (42): 70% (wt/wt) of the cell mass is water, 55% (wt/wt [dry weight]) of the cell mass are proteins, and of that, about half is soluble protein, the estimated amount of CAH in 40 mg of cells (wet weight) is ~0.6 mg. For the APTES-coated cells that translates to a specific activity of 29 μmol/min per mg of CAH purified enzyme. These numbers are almost double the rate observed with CAH enzyme in the literature of 15.7 μmol/min per mg CAH protein (8) and similar to what we determined here for purified enzyme of 27 μmol/min per mg of CAH. This supports previous data presented here showing that the use of the APTES precursor disrupts membranes and allows free diffusion of small molecules into the cell and to the cytoplasmic CAH enzyme, comparable to a pure enzyme in solution.

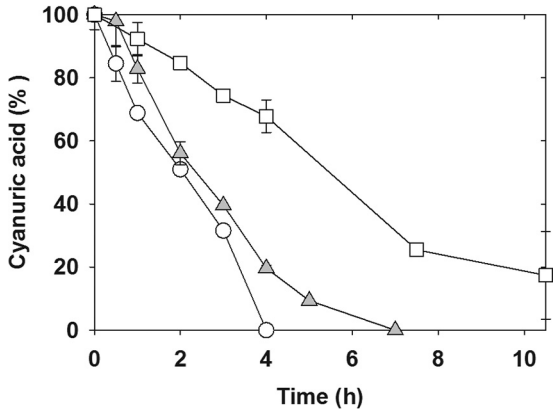

FIG 7 Simulated pool experiment in 4 liters of water at pH 7.6 measuring the decrease in a starting CYA concentration of ~100 ppm over time with treatment by 40 mg of *E. coli* cells as free cells (white squares), APTES gel (gray triangles), or APTES-coated cells (white circles). The symbols show the averages of triplicate determinations, and the error bars show the standard deviations of triplicate determinations.

Using the simulated pool conditions, protection of CAH activity from hypochlorite by APTES was assessed at 1.0, 3.0, and 10.0 ppm hypochlorite (Fig. 8). The data show that APTES gels give the best protection against hypochlorite inactivation but still allow significant diffusion to give good performance, showing almost complete degradation of CYA at 1 ppm hypochlorite and ~30% degradation at 10 ppm, a concentration higher than is typically found in pools. With APTES gels, some hypochlorite inactivation is likely occurring, as indicated by the diminution in rate over time. This is made apparent by the steepest curve shown in Fig. 8, an APTES gel treatment without hypochlorite, which is nearly linear until 80% of the CYA is degraded. This is likely due to the substrate concentration diminishing to near the K_m value for the CAH from *M. thermoacetica* that has been reported to be 14 ppm (110 μM) (8). In contrast, the CAH activity in APTES-coated cells quickly inactivated, and after a small drop in CYA (~5%), no further degradation was observed (top curve in Fig. 8). Furthermore, the increase in CYA degradation rate with dispersed

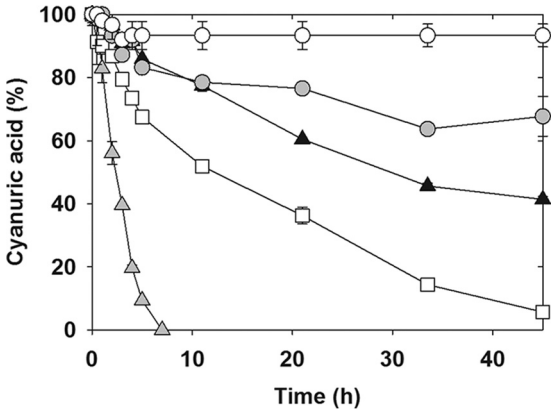

FIG 8 Effect of hypochlorite on cyanuric acid degradation in simulated pool experiment with 4 liters of water at pH 7.6 and containing an initial concentration of CYA of 100 ppm. The percentage of CYA left in solution as a function of time after treatment of 40 mg APTES-coated *E. coli* (CAH) with 1 ppm ClO^- (white circles) and encapsulated *E. coli* (CAH) in APTES gel with no ClO^- (grey triangles) or with 1 ppm ClO^- (white squares), 3 ppm ClO^- (black triangles), and 10 ppm ClO^- (gray circles).

microparticles (Fig. 7 and 8) compared to the rate observed with gel plugs (Fig. 3) indicated that the smaller particle size presents less of a diffusional barrier for CYA entry into the gel. This suggested that there is an opportunity to further optimize the APTES formulation to decrease the diffusional barrier into the gel material while still providing sufficient protection from hypochlorite.

Mechanistic interpretation. The data indicated that the biomaterial developed here has two distinct functionalities: diffusion enhancement (Fig. 9A) and hypochlorite protection (Fig. 9B). Analysis of the degradation rates of cells that were directly reacted with the APTES precursor showed rates comparable to those of purified enzyme, strongly suggesting that the membrane is abrogated and consequently permeable to smaller solutes (Fig. 9A). Despite that, the APTES gel protects and immobilizes the enzyme and as such remains an efficient whole-cell, immobilizing biocatalyst.

APTES-coated cells did not adequately protect the hydrolase against hypochlorite, whereas when cells were encapsulated with APTES (APTES gel), as shown in Fig. 2A, the activity was significantly protected. To clarify this point, we examined the relative rates of reactions and diffusion relevant to the system. The values in the literature for the second-order rate constants of alkyl amines with hypochlorite at neutral pH and ambient temperature are in the range of 10^4 to 10^5 M^{-1} s^{-1} (43). This is very fast for a noncatalyzed chemical reaction, but an accepted value for the diffusional collision rate constant of small molecules with enzymes in water is 10^9 M^{-1} s^{-1} (44). Thus, free diffusion of hypochlorite into cells coated with APTES is orders of magnitude faster than the rates of its reaction with the alkyl amine groups of APTES, and therefore, with the coated cells where diffusion is unimpeded, inactivation prevails. In the case of the gels, it has previously been shown that TEOS gels significantly reduce diffusivity of small molecules (Fig. 1). We hypothesize that the results with hypochlorite in Fig. 8 are due to a proper balancing of diffusivity through the

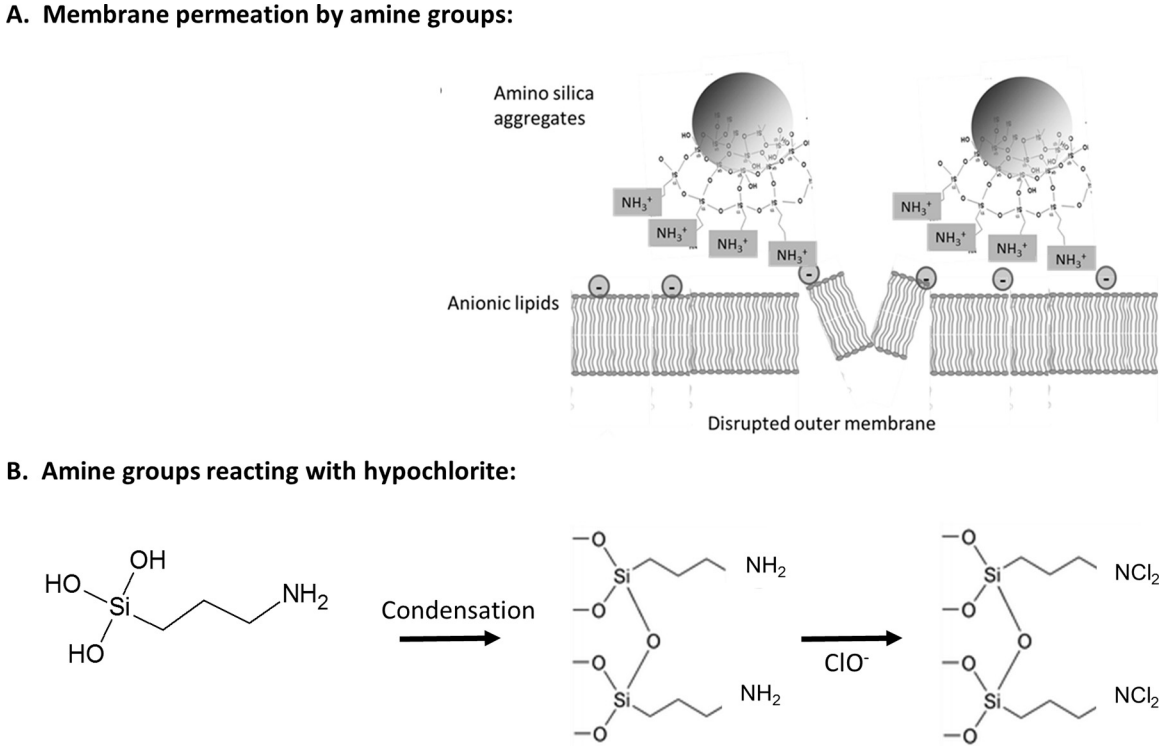

FIG 9 Suggested mechanism of dual functional APTES gels. (A) Illustration of anionic lipids in the cellular membrane interacting electrostatically with the positively charged amine groups, consequently disrupting the outer membrane. (B) Condensation of the APTES precursor to create the amine functionalized silica aggregates and the reaction of the amine groups with hypochlorite to sequester chlorines, delaying enzyme oxidation and enabling sufficient CYA degradation.

silica matrix with the rate of the reaction between hypochlorite and the amine groups of APTES, thus affording an acceptable protection and rate of CYA degradation.

The present work with APTES gels builds on and improves our previous work (25) by (i) enhancing biocatalytic rates significantly by permeabilizing cells and (ii) protecting the intracellular CAH enzyme from damaging oxidation by hypochlorite. There is currently no practical solution for *in situ* removal of cyanuric acid from pool waters, and a biotechnological solution, if effective, could be broadly used. Nonliving genetically engineered microorganisms similar to the ones described here had previously been approved by the U.S. Environmental Protection Agency to apply to soil in an open bioremediation treatment (45). The process described here also contains nonliving organisms and is a closed system. Therefore, it is highly likely to be an acceptable bioremediation material. The major impediment to an effective solution requires cyanuric acid degradation to occur in the presence of chlorine. The present study demonstrates that it is possible to combine rate enhancement and chlorine protection with a modified gel prepared with APTES. Further work will require engineering studies to optimize the mechanical and diffusional properties of functional APTES gels.

MATERIALS AND METHODS

Materials. Tetraethylorthosilicate (TEOS) and 3-aminopropyltriethoxysilane (APTES) were purchased from Sigma-Aldrich Corp. (St. Louis, MO, USA). Silica nanoparticles (NexSil 125-40 with 80-nm diameter) were purchased from Nyacol Nano Technologies Inc. (Ashland, MA, USA). All other reagents and buffers were purchased from Sigma-Aldrich (St. Louis, MO, USA) and were of the highest purity that was commercially available.

Bacterial growth. *E. coli* BL21 expressing cyanuric acid hydrolase from *Moorella thermoacetica* ATCC 39073 (8) was grown at 37°C in LB medium containing 50 μg ml^{-1} kanamycin with vigorous aeration and 0.5 mM isopropyl β-D-1-thiogalactopyranoside (IPTG) added as an inducer at mid-log phase and left overnight at 28°C (shaken overnight). The cells were harvested by centrifugation at 6,370 $\times$ *g* for 10 min and suspended at 0.1 g/ml in phosphate-buffered saline (PBS). Unless stated otherwise, the PBS composition was 10 mM PO_4^{3-}, 137 mM NaCl, and 2.7 mM KCl, and the pH was adjusted to 7.4. All cells were weighed as a nondried pellet, and this is denoted throughout as cell weight (wet weight).

Cyanuric acid hydrolase purification. Cyanuric acid hydrolase enzyme was purified using a modified version of a previously described procedure (25). Cells from 7 g of lyophilized cell paste were resuspended and lysed in 20 ml of 50 mM Tris (pH 7.2) and 200 mM NaCl by three passes through a French press at 10,000 lb/in^2. The sample was clarified by centrifugation at 48,000 $\times$ *g* for 40 min and passed through a 0.45-μm filter prior to loading onto a 5-ml His-Trap HP nickel column (GE Healthcare, Chalfont, United Kingdom) preequilibrated with 50 mM Tris (pH 7.2) and 200 mM NaCl and eluting with a 5% to 100% 0.5 M imidazole gradient. Fractions containing cyanuric acid hydrolase activity were buffer exchanged with a 200 mM NaCl−50 mM Tris-HCl buffer (pH 7.2) to remove imidazole with Amicon 10,000 (10K) or 30K centrifugal filter units.

Cyanuric acid hydrolase activity measurements. Purified enzyme, free cells, and encapsulated cells were assayed for cyanuric acid hydrolase activity by measuring disappearance of cyanuric acid, formation of the product biuret, or both methods in some cases. In the first method, cyanuric acid remaining in reaction mixtures was determined by its complexation with excess melamine (2.5 mg/ml) by adding a 1:1 mixture (volume) of the melamine to the analyte solution. The CYA and melamine complex were quantitatively determined by monitoring turbidity as the apparent absorbance of the mixture at 600 nm. The assay was calibrated against a product formation assay using a high-performance liquid chromatographic (HPLC) (UV) detection method to monitor biuret and was found to give consistent data. Hewlett-Packard HP 1090 liquid chromatograph (Agilent Technologies, Santa Clara, CA, USA) separations were performed by an analytical amino normal-phase column (Alltech Altima column; Grace Davison, Columbia, MD) eluted isocratically with 22:78 phosphate buffer (0.1 M, pH 7.4)/acetonitrile and a flow rate of 0.25 ml/min for 40 min. Cyanuric acid and biuret eluted from the column at 26.8 and 20.0 min, respectively, and were quantitatively determined in comparison to authentic standards with the detector set at 212 nm.

Cyanuric acid hydrolase assays with enzyme treated with hypochlorite were conducted as preincubations with hypochlorite using standard methods of determining time-dependent loss of activity, so that true sensitivity to hypochlorite could be assessed (29). Purified enzyme (30 μM) was incubated with 1 mM (74.4 ppm) and 10 mM (744 ppm) hypochlorite and sampled at different time points (2 to 45 min for 1 mM and 1 to 4 min for 10 mM). Percent activity was compared to CAH activity in the absence of hypochlorite. At each point, 3 μl of the hypochlorite/protein mix was transferred into 140 ppm of CYA (300 μl) to dilute the hypochlorite 1:100, and the reaction proceeded with CYA for 10 min. The reaction was quenched, and the CYA concentration was determined by adding an equal volume of melamine solution (2.5 mg/ml) as described above. In other experiments, hypochlorite inactivation was tested at a very low enzyme concentration (0.2 μg/ml) and 3 ppm hypochlorite to closely mimic levels that would be present in a pool treatment.

Some variations of the standard assay method used with cells in silica gels are described below. A 10-ml solution of CYA (140 ppm) was added to TEOS or APTES gel plugs, free cells, or APTES-coated cells (these will be described below). The final concentration of cells in the gel and suspensions was 0.002 g/ml and was equivalent for all assays. CAH activity was followed at time intervals as described for individual experiments. For APTES and TEOS gels, the clear liquid above gels was withdrawn and filtered through a 0.2-μm Teflon filter, and the analyte was mixed with melamine and assayed as described above. For the cell suspension and APTES-coated cells, the solutions were centrifuged for 1 min at 10,000 rpm and filtered through a 0.2-μm Teflon filter, and the analyte was mixed with melamine and assayed.

Silica gel preparation. Silica gels were prepared by mixing hydrolyzed alkoxides (APTES or TEOS) as cross-linkers with a solution of silica nanoparticles (SNPs) at a volume ratio of 1:7 cross-linker to nanoparticles. Hydrolysis and condensation reactions of the TEOS alkoxide were controlled by adjusting the water/alkoxide ratio and the solution to pH 3.5 for a final concentration of 320 g/liter of hydrolyzed TEOS (22). APTES hydrolysis was carried out by mixing 1.5 ml of APTES solution with 8.5 ml of deionized water on ice for 2 h for a final concentration of 142 g/liter hydrolyzed APTES. Next, the SNP solution, at a concentration of 400 g/liter, was adjusted to pH 7 by adding 1 M hydrochloric acid. Unless stated otherwise, the silica gels were then prepared by mixing 1.75 ml of the silica nanoparticles with 0.25 ml of *E. coli* cells suspended at 0.1 g/ml in PBS at pH 7.4 (or just PBS when no cells were required). To that mixture 0.25 ml of either TEOS or APTES hydrolyzed cross-linker solution was added. The solutions were left to gel for 1.5 h, resulting in silica gel plugs formed at the bottom of 20-ml scintillation glass vials. The resultant gel plug (called the APTES gel) had a volume of 2.25 ml, a diameter of 25 mm, and a thickness of 14 mm. The water content of the gels was approximately 60% (wt/wt). The silica gels were washed with the PBS buffer prior to the activity assays to remove any free cells and cellular materials that were not completely immobilized.

APTES cell coating. The coated cells were prepared using the cross-linker only, without additional SNPs. The cells were prepared using the same cell to cross-linker ratios and volumes as for the silica gels described above. In 20-ml scintillation glass vials, 0.25-ml solution of *E. coli* cells (0.1 g/ml in PBS [pH 7.4]) was mixed with 1.75 ml of PBS and 0.25 ml hydrolyzed APTES and left to react at room temperature while being

gently shaken for 10 min. The result was a suspension of yellow flake-like microparticles, not like the three-dimensional (3D) continuous gel described above. The suspension was then centrifuged at 6,370 × *g* for 10 min to separate any cellular material that may have leaked out of the APTES-coated aggregates. The remaining pellet was resuspended in 2.25 ml PBS to readjust the volume and concentration and was used without further manipulation in the CYA degradation assays. The same procedure for coating cells (the APTES-coated cells) was used for preparation of scanning electron microscopy (SEM) samples, permeability assays, and hypochlorite protection in the simulated pool experiment. All samples were used the same day they were prepared.

Hypochlorite effects on CAH in TEOS gels, APTES gels, and free cells. Hypochlorite-mediated CAH enzyme inactivation was considered to be a function of both hypochlorite and cell concentration, since many cellular molecules are oxidized by hypochlorite and each oxidation removes hypochlorite from the system. In this context, hypochlorite effects on CAH activity are expressed as both the hypochlorite concentration and the mass ratio between hypochlorite and cells when comparing hypochlorite resistance of *E. coli* (CAH) free cells and encapsulated cells in TEOS and APTES gels.

The effect of hypochlorite on *E. coli* (CAH) cells suspended and encapsulated in silica gels is described in detail below. Ten milliliters of hypochlorite solutions ranging from 0 to 1,000 ppm was incubated for 1 h with the following: (i) 0.002 g/ml *E. coli* (CAH) free cells, (ii) 0.002 g/ml *E. coli* (CAH) encapsulated cells in TEOS gels, and (iii) 0.002 g/ml *E. coli* (CAH) encapsulated in APTES gels. The mass ratio of hypochlorite to cells (wet weight) ranged from 0 to 0.5. The suspensions of free cells were centrifuged at 6,370 × *g* for 10 min, resuspended in a 10-ml solution of CYA (140 ppm), and left for 2.0 h (with shaking). The solutions on the TEOS and APTES gel plug samples were discarded, and a 10-ml solution of 140 ppm CYA in PBS was added to the gel plugs and left for 2.0 h (with shaking). Degradation activity was followed by the melamine assay as described above.

SEM imaging. APTES gel samples with *E. coli* cells and *E. coli* cells coated with APTES were prepared as described above with approximately 1 min of gelling time. Then, 30 μl of gel solution was transferred with a pipette onto a small aluminum slide. The slides were dipped in 2.5% (vol/vol) glutaraldehyde for 3 h and dehydrated by a series of ethanol washes (50, 70, 80, 95, and 100% [vol/vol] ethanol). The ethanol was evaporated overnight in a hood. The dried samples on the slides were placed into a carrier and sputter coated with a thin layer of gold-palladium. Scanning electron microscopy (SEM) images were taken by a Hitachi S4700 machine (Schaumburg, IL, USA).

FTIR. Samples for Fourier transform infrared spectroscopy (FTIR) were prepared by reacting APTES gels (without cells) for 2 h with 10-ml solutions of hypochlorite at concentrations equivalent to 0, 50, and 300% molar ratio of hypochlorite to amine functional groups in the gels (14 mM concentration of amine groups). The solutions were then discarded, and the gels were washed three times with deionized water for 10 min each time. The samples were then washed with a 1 M NaOH solution at pH 11 to catalyze an elimination reaction and convert any dichloramino groups to nitrile functional groups. Next, the samples were left to dry in a 130°C oven overnight. They were then crushed with a mortar and pestle, placed on a CaF_2 window, and placed on a temperature-controlled cryostage (FDCS 196; Linkam Scientific Instruments Ltd., United Kingdom). FTIR spectra were collected in the 900 to 4,000 cm^{-1} range with a Nicolet Continuum FTIR microscope, equipped with a deuterated triglycine sulfate (DTGS) detector (Thermo-Nicolet Corp., Madison, WI).

Other analytical methods. Fluorescence measurements were made with propidium iodide. A 25-μl suspension of 0.1 g of *E. coli* (CAH) cells per ml was mixed with 175 μl of PBS and 25 μl of hydrolyzed APTES and TEOS solutions for 10 min. The cells were then centrifuged, and the supernatant was discarded. The cells were resuspended in 200 μl of PBS and doped with 2 μl of a 20 mM solution in dimethyl sulfoxide (DMSO) of the fluorescent probe propidium iodide (PI) for a final concentration of 0.2 mM. A Molecular Devices SpectraMax M5 plate reader (Molecular Devices, Sunnyvale, CA) was used to quantitate the fluorescence intensity. Samples were excited at 535 nm with a cutoff filter at 590 nm, and emission was read from 617 nm. Experiments were performed in triplicate.

For UV spectroscopic measurements, a Beckman 65 spectrophotometer (Beckman Coulter, Inc., Brea, CA) was used. A 3-ml solution of PBS was added to TEOS and APTES gels with encapsulated *E. coli* (CAH) after gelation. The solutions were agitated for an hour on an orbital shaker at 150 rpm, the gels remained intact, and the solution was clear. The PBS solution from the gels was then monitored at 280 nm to observe whether there was a change in absorbance (compared to the PBS stock solution) as a result of molecules leaking out from the cells. Experiments were performed in triplicate. The solutions were further analyzed for protein with a 12.5% (wt/vol) SDS-PAGE gel stained with SimplyBlue SafeStain according to the manufacturer's instructions (Life Technologies). Based on the product specifications, the limit of detection of a specific protein is 10 ng.

The reaction of APTES with hypochlorite was followed by pH and zeta potential measurements. For pH measurements, APTES gels (without cells) were reacted for 2 h with hypochlorite solutions in deionized water at concentrations up to 3 times the molar ratio of hypochlorite to amine functional groups in the gels (14 mM concentration of amine functional groups). The hypochlorite solutions were then discarded, and the gels were washed three times with deionized water for 10 min each time, and the samples were left to dry in a 130°C oven overnight. The samples were then crushed with a mortar and pestle, suspended in 5 ml of deionized water, and measured. The pH measurements were conducted with a Fisher Scientific Accumet basic pH meter (Pittsburgh, PA, USA) calibrated against two standard buffer solutions of pH 4.0 and 10.0. Zeta potential measurements were conducted as follows. The dried and crushed samples were suspended in 5 ml of deionized water and left to settle for 5 min, and a 1-ml sample of suspension from the top of the glass vial was measured. The samples were measured by a Zetasizer Nanosystem (Malvern Instruments, Southborough, MA), and the zeta potential was deduced from the mobility of the particles by using the Smoluchowski equation (46).

Simulated pool experiments testing the effects of hypochlorite on CYA degradation. In 4-liter Erlenmeyer flasks, pool water conditions were created with buffered water (5 mM PO_4^{3-}, 68 mM NaCl, and 1.35 mM KCl) adjusted to pH 7.6 and containing 100 ppm CYA. Hypochlorite concentrations added were typical of, or somewhat higher than, those found in pools: 0.0, 1.0, 3.0, and 10.0 ppm ClO^-. Degradation of CYA was followed in three treatments that all contained 40 mg of cells to allow direct comparisons. In treatment 1, treatment for free cells, 0.4 ml of a 0.1-g/ml *E. coli* (CAH) cell suspension in PBS was added directly to the flasks. In treatment 2, treatment for APTES-coated cells, 0.4 ml of free cells (0.1 g/ml) was mixed with 3.6 ml of PBS and 0.4 ml of hydrolyzed APTES for 10 min and added to the flasks. In treatment 3, treatment for APTES gel of *E. coli* (CAH) cells, 0.4 ml of free cells was mixed with 3.6 ml SNP (400 g/liter) and 0.4 ml of hydrolyzed APTES. In the next step of treatment 3, the solutions were left to gel as a thin film on a 60-mm-diameter plastic petri dish for 1.5 h. In the last step of treatment 3, the soft gel was then scraped and added to the flasks creating a cloudy suspension of microparticles. The flasks were gently stirred (~60 rpm) with a magnetic stirrer to keep cells suspended and mimic a pool skimmer filter, which would promote continuous mixing. The decrease in CYA concentration was monitored over time by extracting 1-ml aliquots, filtering through a 0.2-μm Teflon filter, and assaying for CYA with the melamine assay as described previously.

SUPPLEMENTAL MATERIAL

Supplemental material for this article may be found at http://mbio.asm.org/lookup/suppl/doi:10.1128/mBio.01477-15/-/DCSupplemental.

Figure S1, TIF file, 1.9 MB.
Figure S2, TIF file, 0.1 MB.
Figure S3, TIF file, 0.1 MB.

ACKNOWLEDGMENTS

This research was supported by Vaadia-BARD Postdoctoral Fellowship award no. FI-516-2014 from BARD, the United States-Israel Binational Agricultural Research and Development Fund, a MnDRIVE postdoctoral fellowship from the BioTechnology Institute, and funding from the BioTechnology Institute under the Synthetic Ecology Initiative and from the MnDRIVE Transdisciplinary Initiative of the University of Minnesota.

We thank Goeun Heo for help with SEM imaging.

Lawrence P. Wackett and Alptekin Aksan own equity in and are entitled to royalties from Minnepura Technologies, Inc., a company involved in the development, commercialization, and marketing of patented encapsulated biological platforms for water treatment. The University of Minnesota also has equity and royalty interest in Minnepura. These interests have been reviewed and managed by the University of Minnesota in accordance with its conflict of interest policies.

REFERENCES

1. **Chen RR**. 2007. Permeability issues in whole-cell bioprocesses and cellular membrane engineering. Appl Microbiol Biotechnol **74:**730–738. http://dx.doi.org/10.1007/s00253-006-0811-x.
2. **Zajkoska P, Rebroš M, Rosenberg M**. 2013. Biocatalysis with immobilized *Escherichia coli*. Appl Microbiol Biotechnol **97:**1441–1455. http://dx.doi.org/10.1007/s00253-012-4651-6.
3. **Huthmacher K, Most D**. 2005. Cyanuric acid and cyanuric chloride, p 9–10. *In* Ullmann's encyclopedia of industrial chemistry. John Wiley and Sons, Inc, New York, NY.
4. **Canelli E**. 1974. Chemical, bacteriological, and toxicological properties of cyanuric acid and chlorinated isocyanurates as applied to swimming pool disinfection: a review. Am J Public Health **64:**155–162. http://dx.doi.org/10.2105/AJPH.64.2.155.
5. **Anderson JR**. 1965. A study of the influence of cyanuric acid on the bactericidal effectiveness of chlorine. Am J Public Health **55:**1629–1637. http://dx.doi.org/10.2105/AJPH.55.10.1629.
6. **Fitzgerald GP, DerVartanian ME**. 1967. Factors influencing the effectiveness of swimming pool bactericides. Appl Microbiol **15:**504–509.
7. **Murphy JL, Arrowood MJ, Lu X, Hlavsa MC, Beach MJ, Hill VR**. 2015. Effect of cyanuric acid on the inactivation of Cryptosporidium parvum under hyperchlorination conditions. Environ Sci Technol **49:**7348–7355. http://dx.doi.org/10.1021/acs.est.5b00962.
8. **Li Q, Seffernick JL, Sadowsky MJ, Wackett LP**. 2009. Thermostable cyanuric acid hydrolase from *Moorella thermoacetica* ATCC 39073. Appl Environ Microbiol **75:**6986–6991. http://dx.doi.org/10.1128/AEM.01605-09.
9. **Seffernick JL, Erickson JS, Cameron SM, Cho S, Dodge AG, Richman JE, Sadowsky MJ, Wackett LP**. 2012. Defining sequence space and reaction products within the cyanuric acid hydrolase (AtzD)/barbiturase protein family. J Bacteriol **194:**4579–4588. http://dx.doi.org/10.1128/JB.00791-12.
10. **Cho S, Shi K, Seffernick JL, Dodge AG, Wackett LP, Aihara H**. 2014. Cyanuric acid hydrolase from *Azorhizobium caulinodans* ORS 571: crystal structure and insights into a new class of ser-lys dyad proteins. PLoS One **9:**e99349. http://dx.doi.org/10.1371/journal.pone.0099349.
11. **Peat TS, Balotra S, Wilding M, French NG, Briggs LJ, Panjikar S, Cowieson N, Newman J, Scott C**. 2013. Cyanuric acid hydrolase: evolutionary innovation by structural concatenation. Mol Microbiol **88:**1149–1163. http://dx.doi.org/10.1111/mmi.12249.
12. **Hawkins CL, Pattison DI, Davies MJ**. 2003. Hypochlorite-induced oxidation of amino acids, peptides and proteins. Amino Acids **25:**259–274. http://dx.doi.org/10.1007/s00726-003-0016-x.
13. **Schraufstätter IU, Browne K, Harris A, Hyslop PA, Jackson JH, Quehenberger O, Cochrane CG**. 1990. Mechanisms of hypochlorite injury of target cells. J Clin Invest **85:**554–562. http://dx.doi.org/10.1172/JCI114472.
14. **Baker RWR**. 1947. Studies on the reaction between sodium hypochlorite and proteins: 1. Physico-chemical study of the course of the reaction. Biochem J **41:**337–342. http://dx.doi.org/10.1042/bj0410337.
15. **Gray MJ, Wholey W-Y, Jakob U**. 2013. Bacterial responses to reactive chlorine species. Annu Rev Microbiol **67:**141–160. http://dx.doi.org/10.1146/annurev-micro-102912-142520.
16. **Hofbauer S, Gruber C, Pirker KF, Sündermann A, Schaffner I, Jakopitsch C, Oostenbrink C, Furtmüller PG, Obinger C**. 2014. Transiently produced hypochlorite is responsible for the irreversible inhibition of chlorite dismutase. Biochemistry **53:**3145–3157. http://dx.doi.org/10.1021/bi500401k.
17. **Avnir D, Braun S, Lev O, Ottolenghi M**. 1994. Enzymes and other proteins entrapped in sol-gel materials. Chem Mater **6:**1605–1614. http://dx.doi.org/10.1021/cm00046a008.
18. **Avnir D, Coradin T, Lev O, Livage J**. 2006. Recent bio-applications of sol-gel materials. J Mater Chem **16:**1013–1030. http://dx.doi.org/10.1039/B512706H.
19. **Duetz WA, Van Beilen JB, Witholt B**. 2001. Using proteins in their natural environment: potential and limitations of microbial whole-cell hydroxylations in applied biocatalysis. Curr Opin Biotechnol **12:**419–425. http://dx.doi.org/10.1016/S0958-1669(00)00237-8.
20. **Ni Y, Chen RR**. 2004. Accelerating whole-cell biocatalysis by reducing outer membrane permeability barrier. Biotechnol Bioeng **87:**804–811. http://dx.doi.org/10.1002/bit.20202.
21. **Meunier CF, Dandoy P, Su B-L**. 2010. Encapsulation of cells within silica matrixes: towards a new advance in the conception of living hybrid materials. J Colloid Interface Sci **342:**211–224. http://dx.doi.org/10.1016/j.jcis.2009.10.050.
22. **Mutlu BR, Yeom S, Tong H-W, Wackett LP, Aksan A**. 2013. Silicon alkoxide cross-linked silica nanoparticle gels for encapsulation of bacterial biocatalysts. J Mater Chem A **1:**11051–11060. http://dx.doi.org/10.1039/c3ta12303k.
23. **Livage J, Coradin T, Roux C**. 2001. Encapsulation of biomolecules in silica gels. J Phys Condens Matter **13:**R673–R691. http://dx.doi.org/10.1088/0953-8984/13/33/202.
24. **Mutlu BR, Yeom S, Wackett LP, Aksan A**. 2015. Modelling and optimization of a bioremediation system utilizing silica gel encapsulated whole-cell biocatalyst. Chem Eng J **259:**574–580. http://dx.doi.org/10.1016/j.cej.2014.07.130.
25. **Yeom S, Mutlu B, Aksan A, Wackett LP**. 2015. Bacterial cyanuric acid hydrolases for water treatment. Appl Environ Microbiol **81:**6660–6668. http://dx.doi.org/10.1128/AEM.02175-15.
26. **Milović NM, Wang J, Lewis K, Klibanov AM**. 2005. Immobilized N-alkylated polyethylenimine avidly kills bacteria by rupturing cell membranes with no resistance developed. Biotechnol Bioeng **90:**715–722.
27. **Hong S, Leroueil PR, Janus EK, Peters JL, Kober M-M, Islam MT, Orr BG, Baker JR, Jr, Banaszak Holl MM**. 2006. Interaction of polycationic polymers with supported lipid bilayers and cells: nanoscale hole formation and enhanced membrane permeability. Bioconjug Chem **17:**728–734. http://dx.doi.org/10.1021/bc060077y.
28. **Burckhardt B-C, Thelen P**. 1995. Effect of primary, secondary and tertiary amines on membrane potential and intracellular pH in *Xenopus laevis* oocytes. Pflugers Arch **429:**306–312. http://dx.doi.org/10.1007/BF00374144.
29. **Walsh C**. 1979. Acyl transfers to water: endopeptidases and exopeptidases, p 53–107. *In* Enzymatic reaction mechanisms. WH Freeman & Co, New York, NY.
30. **Reátegui E, Reynolds E, Kasinkas L, Aggarwal A, Sadowsky MJ, Aksan A, Wackett LP**. 2012. Silica gel-encapsulated AtzA biocatalyst for atrazine biodegradation. Appl Microbiol Biotechnol **96:**231–240. http://dx.doi.org/10.1007/s00253-011-3821-2.
31. **Lopez-Amoros R, Comas J, Vives-Rego J**. 1995. Flow cytometric assessment of *Escherichia coli* and *Salmonella typhimurium* starvation-survival in seawater using rhodamine 123, propidium iodide, and oxonol. Appl Environ Microbiol **61:**2521–2526.
32. **Dolezalova E, Lukes P**. 2015. Membrane damage and active but nonculturable state in liquid cultures of Escherichia coli treated with an atmospheric pressure plasma jet. Bioelectrochemistry **103:**7–14. http://dx.doi.org/10.1016/j.bioelechem.2014.08.018.
33. **Walev I, Bhakdi SC, Hofmann F, Djonder N, Valeva A, Aktories K, Bhakdi S**. 2001. Delivery of proteins into living cells by reversible membrane permeabilization with streptolysin-O. Proc Natl Acad Sci USA **98:**3185–3190. http://dx.doi.org/10.1073/pnas.051429498.
34. **Monaghan-Benson E, Wittchen ES**. 2011. In vitro analyses of endothelial cell permeability. Methods Mol Biol **763:**281–290. http://dx.doi.org/10.1007/978-1-61779-191-8_19.
35. **Kovacic P, Lowery MK, Field KW**. 1970. Chemistry of N-bromamines and N-chloramines. Chem Rev **70:**639–665. http://dx.doi.org/10.1021/cr60268a002.
36. **Morris JC**. 1966. The acid ionization constant of HOCl from 5 to 35°. J Phys Chem **70:**3798–3805. http://dx.doi.org/10.1021/j100884a007.

37. **Kim J, Seidler P, Wan LS, Fill C**. 2009. Formation, structure, and reactivity of amino-terminated organic films on silicon substrates. J Colloid Interface Sci **329:**114–119. http://dx.doi.org/10.1016/j.jcis.2008.09.031.
38. **Worley SD, Wojtowicz JA**. 2004. *N*-Halamines, p 98–122. *In* Kirk-Othmer encyclopedia of chemical technology. John Wiley & Sons, Inc, New York, NY.
39. **Lambert JB, Shurvell HF, Verbit L, Cooks GR, Stout GH**. 1976. Organic structural analysis. Macmillan Publishing Co, Inc, New York, NY.
40. **Foschiera JL, Pizzolato TM, Benvenutti EV**. 2001. FTIR thermal analysis on organofunctionalized silica gel. J Braz Chem Soc **12:**159–164. http://dx.doi.org/10.1590/S0103-50532001000200006.
41. **Silverstein RM, Webster FX, Kiemle D, Bryce DL**. 2014. Spectrometric identification of organic compounds. John Wiley & Sons, Hoboken, NJ. http://dx.doi.org/10.1021/ed039p546.
42. **Maaloe O, Ingraham GL, Maaloe O, Neidhardt FC**. 1983. Growth of the bacterial cell. Sinauer Association, Inc., Sunderland, MA.
43. **Deborde M, Von Gunten U**. 2008. Reactions of chlorine with inorganic and organic compounds during water treatment—kinetics and mechanisms: a critical review. Water Res **42:**13–51. http://dx.doi.org/10.1016/j.watres.2007.07.025.
44. **Williamson M**. 2011. How proteins work. Garland Science, New York, NY.
45. **Strong LC, McTavish H, Sadowsky MJ, Wackett LP**. 2000. Field-scale remediation of atrazine-contaminated soil using recombinant *Escherichia coli* expressing atrazine chlorohydrolase. Environ Microbiol **2:**91–98. http://dx.doi.org/10.1046/j.1462-2920.2000.00079.x.
46. **Hunter RJ**. 2013. Zeta potential in colloid science: principles and applications, vol **2**. Academic Press, San Diego, CA.